Variance Stabilizing Transformations in the Reduction of Poisson Noise in 3D Nuclear Medicine Images

Edward Flórez Pacheco[1], Sergio Shiguemi Furuie[1]

School of Engineering, University of São Paulo, Brazil

Abstract

Nuclear medicine (NM) is a modality of medical imaging that uses radioactive materials to provide information about the functioning of a person's specific organs. However, the NM images are characterized by presenting poor signal to noise ratio, related to low counts and to Poisson noise because of the stochastic nature of the attenuation processes (absorption and scattering). These kinds of images depict regions with high counting photons that are created by a group of cells that have a faster metabolism indicating physiological changes. This phenomenon could suggest the presence of a malignant neoplasia (tumor). Hence, before applying any technique for determining metabolic rates, first it is necessary to define the region of interest (ROI). For this purpose, segmentation techniques were used based on the Fuzzy Connectedness theory. It is possible to improve the efficiency of the segmentation stage by using appropriate filters for the treatment of the Poisson noise. This study used anthropomorphic phantoms of the left ventricle of the heart. A NM exam was simulated using GATE platform with the phantom coupled to the PET scanner recreated. Then, the projections obtained were reconstructed using the STIR platform. Several studies have shown the effectiveness of the Anscombe Transformation in the stabilization of the variance of NM images. However, in this paper other approaches like Bartlett and Freeman & Tukey were used and compared to the original method of transformation. Wiener filter was used in combination with all the types of transformations tested. Freeman & Tukey / Wiener filter improve the efficiency of the segmentation stage compared to the other two filters. In the near future, this procedure will be applied in real 3D images.

1. Introduction

Clinically, it is known the importance for the specialist to have knowledge of the location and subsequently to detect functional and metabolic alterations in a particular area of the body, especially because they precede anatomical alterations [1; 2].

Thus, the role of the Nuclear Medicine is currently diagnostic, prognostic and control, with a very significant potential for therapeutic aspects in an attempt to cure diseases and some forms of cancer by radiotherapy [3].

Due to the lack of computational tools and techniques to assess and study the dynamics of processes from images of Nuclear Medicine is intended to contribute with new perspectives, new approaches and tools to assist, facilitate and improve the work of specialists.

2. Methods

Our work is constituted by a sequence of interrelated modules and steps which were implemented as part of the study. The steps will be detailed below:

2.1. Acquisition of 3D simulated images

The research involves no new experiments with animals or humans, since numerical phantoms were used.

(a) NCAT-4D Phantom

We were provided by the Computer Service of the Heart Institute of São Paulo (InCor) some phantoms simulated with NCAT-4D. Figure 1 shows the simulation of the Left Ventricle of the Heart along with structures of the ribcage. This phantom (Figure 1) is conformed for a set of 10 frames, each frame has 20 slices.

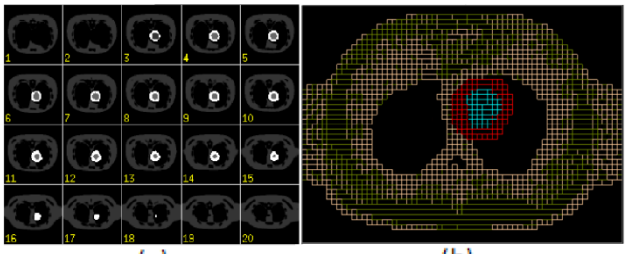

Figure 1. Phantom simulated using the 4D-NCAT. (a) Projections of 2D slices of the left ventricle inside the ribcage using XMedCon software, (b) volume generated with GATE platform.

(b) Modeling of PET tomograph (BiographTM)

According to the manuals and data sheets of the equipment, provided by the Nuclear Medicine Center of São Paulo, we identified the most relevant data and dimensions of the architecture of the scanner Siemens brand, model BiographTM. These data were incorporated in the simulation files (dimensions of the scanner, the type of detectors, the detectors distribution, etc.), and generating a near tomograph used in the acquisition process.

(c) Realistic Simulation Process

Using the GATE platform has been possible to generate realistic projections PET with an outstanding proximity to those generated with the real equipment PET, using for this purpose the Monte Carlo simulation.

Therefore, the anthropomorphic phantom NCAT-4D was coupled into the GATE and positioned in the center of the tomograph BiographTM modeled (Figure 2), to execute the simulated PET exam and get the projections as product of the acquisition process.

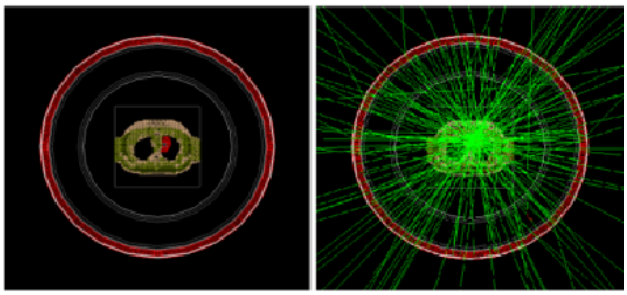

Figure 2. Simulated PET exam using GATE platform (a) NCAT-4D phantom coupled into the tomograph BiographTM, (b) beginning of the simulation.

We used 1 MBq of activity in the simulation and it had a duration aprox. of 75 hours in a high-performance computer (Dell Brand, Model Precision T7600, Intel Xeon E5-2620, @ 2.00GHz 6-core, OS 64 bits, 32 GB of RAM).

Subsequently, the STIR software was used as a 3D reconstruction platform on the display, manipulation and in the reconstruction process of the 3D PET images. Specifically, the OSEM iterative reconstruction method was used for this purpose.

2.2. Filtering of 3D images

According to the literature, it is known that PET images are corrupted by quantum noise that is dependent of the signal and can be modeled by a Poisson statistical distribution [4].

The method considered in this study performs a restoration in the images utilizing, as a first step, the Variance Stabilizing Transformation (VST) and the Wiener filter to reduce the Poisson noise.

Subsequently, we used the Inverse Transform (IT) for the enhancement of the structures of interest in the filtered image.

(i) Variance Stabilizing transformation (VST)

The VST is a data transformation that aims to simplify considerations in data analysis when the assumption of a linear model is not satisfied [5].

For example, the Anscombe transform (AT) is a nonlinear transformation that allows to change the quantum noise of a digital image that is signal dependent into a noise approximately independent of the signal, additive, Gaussian, with zero mean and unit variance [4]. There are similar alternatives such as the Bartlett transform [6] and the Freeman & Tukey transform [7], which has been implemented and tested.

According to [8], given the random variable $\tilde{U}_i$ with Poisson statistical distribution, we can express the AT this random variable by using the equation (1). Similarly, the random variable representing the $\tilde{U}_i$ transformed by Bartlett and Freeman & Tukey transform are expressed by equations (2) and (3), respectively.

$$\tilde{Z}_i = 2 \cdot \sqrt{\tilde{U}_i + \frac{3}{8}} \qquad (1)$$

$$\tilde{Z}_i = 2 \cdot \sqrt{\tilde{U}_i + \frac{1}{2}} \qquad (2)$$

$$\tilde{Z}_i = \sqrt{\tilde{U}_i} + \sqrt{\tilde{U}_i + 1} \qquad (3)$$

This new variable $\tilde{Z}_i$ of the above equations can be represented by an additive model [5] as shown in equation (4):

$$\tilde{Z}_i = 2 \cdot \sqrt{\tilde{U}_i + \frac{1}{8}} + \tilde{N}_i = \tilde{S}_i + \tilde{N}_i \qquad (4)$$

with $\tilde{N}_i$ being a noise approximately independent of the signal $\tilde{S}_i$, described by a Gaussian distribution with zero mean and variance unit.

(ii) Wiener filter

The Wiener Filter off [9] is an optimal linear filter and can be used for filtering the additive Gaussian noise. An estimate without noise $\hat{s}_i$ for z_i is obtained using the Wiener filter given by the equation:

$$\hat{s}_i = E[\tilde{S}_i] + \frac{\sigma^2_{\hat{s}_i}}{\sigma^2_{\hat{s}_i} + 1}(\tilde{Z}_i - E[\tilde{S}_i]) \qquad (5)$$

where the mean $E[\tilde{S}_i]$ and the variance $\sigma^2_{\hat{s}_i}$ of $\hat{s}_i$ are local measures and may be estimated in practice from the image to be filtered.

(iii) Inverse Transform (IT)

After the filtering step, we applied the Inverse transform in order to have an estimate of the degraded image without the Poisson noise. We can express the IT on $\hat{s}_i$ by the equation:

$$\hat{b}_i = \frac{1}{4} . \hat{s}_i^2 - \frac{3}{8} \quad (6)$$

Figure 3 shows two-dimensional slices of a portion of the left ventricle simulated with NCAT-4D. The first slice shown in (a) contains Poisson noise and the other slice shown in (b) is the resulting slice after the execution of Freeman & Tukey / Wiener filter.

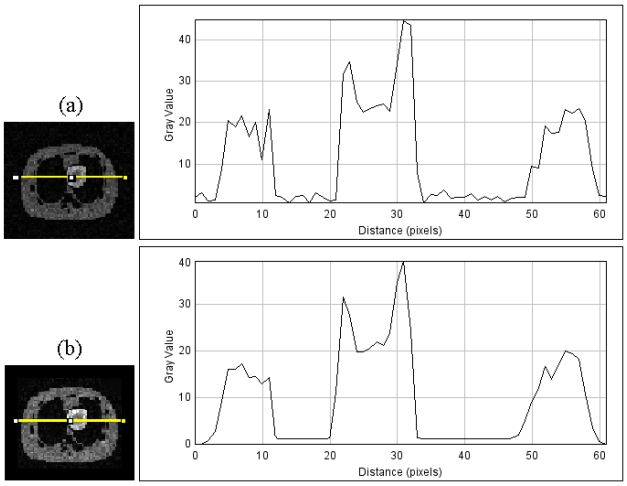

Figure 3. Profile (center horizontal line) of (a) Image with Poisson noise and (b) Image filtered.

2.3. 3D segmentation of the ROI

Segmentation is a process of decomposing an image into regions or objects [10], making the identification of spels (pixels or voxels) that are part of the region of interest (ROI) selected by the user.

The segmentation process applied in this work is based on the concept of Fuzzy Connectedness (FC) using the approach of dynamic weights [11].

One of the fundamental concepts of the FC theory and the segmentation process is the factor of Affinity. Based on the concept of affinity, it is possible to find a connectivity between any two spels, c and d, from a number of local affinities between the pair of elements [11]. It is clear that there are several paths passing only by unit adjacencies that can combine these two spels. Assuming that $p_{c,d} = \langle s_1, s_2, \dots, s_N \rangle$ is one path between $s_1 = c$ and $s_N = d$, where s_i is N spels adjacent to each other pairs, the affinity of this path is given by:

$$\mu_K(p_{c,d}) = \min_{1<i<N}(\mu_k(s_{i-1}, s_i)) \quad (7)$$

Thus, the selection of the higher affinity will be the best representation of the global connectivity. Therefore, assuming that $P_{c,d}$ is a set of all paths p, the global connectivity between c and d is defined as:

$$\mu_K(c, d) = \max_{p \in P_{c,d}}(\min_{1<i<N}(\mu_k(s_{i-1}, s_i))) \quad (8)$$

Then, three fundamental properties integrate the Affinity element: adjacency (μ_α), homogeneity (μ_ψ), and intensity (μ_ϕ) [10].

$$\mu_k = \mu_\alpha(c, d). g(\mu_\psi(c, d), \mu_\phi(c, d)) \quad (9)$$

Since the adjacency relationship $\mu_\alpha(c, d)$ indicates the spatial proximity between the elements evaluated, if c and d are neighbors the adjacency Fuzzy is unitary. Then, the affinity is expressed as:

$$\mu_k = g(\mu_\psi(c, d), \mu_\phi(c, d)) \quad (10)$$

Thus, the affinity for each pair of spels c and d of a path $p_{c,d}$ is expressed by:

$$\mu_k(c, d) = w_1 \mu_\phi(c, d) + w_2 \mu_\psi(c, d) \quad (11)$$

$$\mu_\psi(c, d) = \exp\left[-\frac{1}{2}\left(\frac{|f(c)-f(d)|-m_1}{s_1}\right)^2\right] \quad (12)$$

$$\mu_\phi(c, d) = \exp\left[-\frac{1}{2}\left(\frac{\left(\frac{f(c)+f(d)}{2}\right)-m_2}{s_2}\right)^2\right] \quad (13)$$

$$w_1 = \frac{\mu_\phi(c,d)}{\mu_\phi(c,d)+\mu_\psi(c,d)}, \quad w_2 = 1 - w_1 \quad (14)$$

where m_1 and s_1 are the mean and standard deviation of the local homogeneity of the object. On the other hand, m_2 and s_2 are the mean and standard deviation of the intensities of the object, respectively. The weights w_1 and w_2 are adjusted for each pair of elements c and d belonging to the same path.

3. Results

Table 1 shows the results of evaluation applied on 10 LV volumes from NCAT-4D simulated using three different metrics: True Positive (TP), False Positive (FP) and Maximum Distance (Max_dist) [12].

The processes of simulation, reconstruction, filtering (Anscombe/Wiener, Bartlett/Wiener and Freeman&Tukey /Wiener filters) and segmentation (Fuzzy Connectedness with Dynamic Weights) were followed.

Table 1. Results and consolidation of the tests in the NCAT-4D phantom using the three diferentes filters.

Frame	Process Seq. (Filters)	TP (%)	FP (%)	MaxDist
1	Volume w/Poisson noise	85,83	6,36	5
	Anscombe/Wiener	92,74	3,02	3
	Barlett/Wiener	91,45	2,95	3
	Freeman&Tukey/Wiener	93,84	1,98	2
2	Volume w/Poisson noise	91,93	5,82	5
	Anscombe/Wiener	93,54	2,65	2
	Barlett/Wiener	92,89	3,71	3
	Freeman&Tukey/Wiener	93,86	1,73	2
3	Volume w/Poisson noise	87,64	5,89	5
	Anscombe/Wiener	92,58	2,56	3
	Barlett/Wiener	91,49	3,62	3
	Freeman&Tukey/Wiener	93,19	1,32	1
4	Volume w/Poisson noise	92,95	7,59	5
	Anscombe/Wiener	93,88	2,19	3
	Barlett/Wiener	93,14	3,86	3
	Freeman&Tukey/Wiener	94,08	1,48	2
5	Volume w/Poisson noise	87,83	6,79	5
	Anscombe/Wiener	93,08	2,14	3
	Barlett/Wiener	91,93	3,71	3
	Freeman&Tukey/Wiener	93,69	1,18	2
6	Volume w/Poisson noise	93,23	7,04	5
	Anscombe/Wiener	94,57	2,84	2
	Barlett/Wiener	93,42	3,86	3
	Freeman&Tukey/Wiener	95,27	0,97	1
7	Volume w/Poisson noise	85,52	5,29	5
	Anscombe/Wiener	92,51	2,39	3
	Barlett/Wiener	92,45	3,07	3
	Freeman&Tukey/Wiener	93,91	1,21	2
8	Volume w/Poisson noise	87,13	6,86	5
	Anscombe/Wiener	92,76	2,58	3
	Barlett/Wiener	91,78	3,87	3
	Freeman&Tukey/Wiener	94,98	0,87	1
9	Volume w/Poisson noise	91,42	7,39	5
	Anscombe/Wiener	94,74	2,78	2
	Barlett/Wiener	92,58	3,45	3
	Freeman&Tukey/Wiener	94,74	1,49	2
10	Volume w/Poisson noise	93,14	5,59	5
	Anscombe/Wiener	94,21	2,35	3
	Barlett/Wiener	93,23	3,28	3
	Freeman&Tukey/Wiener	95,23	0,67	1
Consolidated	**Volume w/Poisson noise**	**89.53 ± 4.71**	**6.34 ± 1.82**	**5 pixels**
	Anscombe/Wiener	**93.49 ± 1.31**	**2.25 ± 0.85**	**3 pixels**
	Barlett/Wiener	**92.07 ± 1.74**	**3.18 ± 0.94**	**3 pixels**
	Freeman&Tukey/Wiener	**94.88 ± 1.12**	**1.34 ± 0.68**	**2 pixels**

4. Discussion and conclusion

The effectiveness of the Anscombe/Wiener filter is known in the imaging of NM. However, in this work other approaches were tested with encouraging results. We intend to conduct additional experiments to evaluate statistically this improvement.

Based on the results of the evaluation of the left ventricle volumes from NCAT-4D, we can indicate that the Freeman&Tukey/Wiener filter gave the best results, considering the quality of the segmentation as a functional criterion.

The results of the segmentation using the Freeman & Tukey / Wiener filter proved to be quite satisfactory. It has been obtained 1.34% of FP and 94.88% of TP at the end of the sequence of processing.

This work highlighted the importance of the filtering step, being a prime requirement for a better segmentation.

In order to give greater support to our processing framework, real PET images will be used in future tests.

Acknowledgements

LEB-EPUSP (Biomedical Engineering Laboratory-Politecnical School of the University of São Paulo), **InCor** (Heart Institute of São Paulo), **CMN-FMUSP** (Center of Nuclear Medicine of the Faculty of Medicine - University of São Paulo), **FAPESP** (São Paulo Research Foundation).

References

[1] De Almeida JP, Trindade MV, Gomes D, Fernandes CDO que é Medicina Nuclear? www.rxinfo.com.br/, 2002.

[2] Robilotta CC. A tomografia por emissão de pósitrons: uma nova modalidade na medicina nuclear brasileira. Rev Panam Salud Publica 2006; 20:134–42.

[3] Carrió I, Gonzáles P, Estorch M, Canessa J, Mitjavila M, Massardo T. Medicina nuclear: aplicaciones clínicas. Editorial Masson S.A., España, 2003.

[4] Inouye T. Square root transform for the analysis of quantum fluctuationes in spectrum data. Nuclear Instruments and Methods 91. 1970.

[5] Allen D. Variance stabilization transformations. University of Kentucky. 2013.

[6] Bartlett MS. The square root transformation in analysis of variance. J R Statist Soc 1936;Suppl 3(1): 68-78.

[7] Freeman MF, Tukey JW. Transformations related to the angular and the square root. Institute of Mathematical Statistics – Princeton University. 1972.

[8] Anscombe FJ. The transformation of Poisson, binomial and negative binomial data. Biometrika 1948;15: 246-254.

[9] Lee JS. Digital image enhancement and noise filtering by use of local statistics. IEEE Transactions on Pattern Analysis and Machine Intelligence 1980;PAMI-2:165-168.

[10] Gonzales RC; Woods RE. Digital Image Processing. 3rd ed, New Jersey, Pearson Prentice Hall, 2008. Chap.9 – Morphological Image Processing.

[11] Nyúl ALG, Falcão AX, Udupa JK. Fuzzy-connected 3D image segmentation at interactive speeds. Elsevier on Graphical Models 2002;64:259-281.

[12] Udupa KJ, LaBlanc RV, Schmidt H. A methodology for evaluating image segmentation algortihms. 2002

Address for correspondence.

Edward Flórez Pacheco
Laboratório de Engenharia Biomédica. Departamento de Telecomunicações e Controle. Escola Politécnica da Universidade de São Paulo. Av. Prof. Luciano Gualberto, Travessa 3, 158 – Sala D2-06. CEP 05508-970 SP -São Paulo – Brasil.
edward.florez@usp.br